Development of a simple SERS substrate for the detection of pollutants and nanoplastics

Lara Mikac[a*], Hrvoje Gebavi[a], Justin Perrault[b], Mile Ivanda[a*]

[a]*Laboratory for Molecular Physics and Synthesis of New Materials, Ruđer Bošković Institute, Bijenička 54, Zagreb, Croatia*

[b]*Polytech Nantes, University of Nantes, Rue Christian Pauc, 44300 Nantes, France*

Abstract.

This study investigates the development and characterisation of Ag- and Au-coated silicon filter substrates developed for surface-enhanced Raman spectroscopy (SERS) applications. Silver nanoparticles were synthesised by immersing silicon filters in an $AgNO_3$ solution, with the immersion time playing a crucial role in nanoparticle distribution and SERS efficiency. The highest performance was observed at an immersion time of 30–60 minutes and allowed the detection of 4-mercaptobenzoic acid (4-MBA) at nanomolar concentrations. To improve stability and tunability, gold was sputtered onto the Ag-coated substrates. Optimal performance was achieved with 6 minutes of Au sputtering, which allowed picomolar sensitivity for 4-MBA and micromolar detection of melamine. These substrates were further tested for the detection of polystyrene (PS) and polyethylene (PE) nanoplastic particles by Raman mapping with particles down to 50 nm. The successful identification showed great potential for the micro-Raman analysis of nanomaterials. The results emphasise the high sensitivity, versatility and ease of production of the SERS substrates and highlight their potential for applications in environmental and food monitoring, especially for the detection of nanoplastics.

Keywords: silver, gold, 4-mercaptobenzoic acid (4-MBA), melamine, nanoplastic (NP), polyethylene (PE), polystyrene (PS)

1. Introduction

In recent decades, surface-enhanced Raman spectroscopy (SERS) has become a powerful analytical technique for the sensitive and selective detection of molecules at extremely low concentrations [1-3]. This ability is due to the significant enhancement of Raman signals that occurs when analytes are in close proximity to nanostructured metallic surfaces [4, 5]. Essentially, SERS utilises the phenomenon of localised surface plasmon resonance (LSPR), which occurs when light interacts with the collective vibrations of conduction electrons on the surface of nanoscale metallic structures. Among the many materials being explored for use as SERS substrates, silver nanoparticles (NPs) have attracted considerable attention [6-8]. This is due to their extraordinary plasmonic properties, which are characterised by collective electron oscillations in response to incident light and can be fine-tuned by changing the size, shape, and arrangement of these nanoparticles. Therefore, Ag NPs serve as versatile building blocks for the fabrication of SERS-active surfaces and allow precise control over their plasmonic properties. Gold NPs are often integrated into SERS substrates as their plasmonic band position and potentially higher chemical affinity for certain analytes can significantly increase the intensity of the Raman signal [9]. In addition, Au NPs offer excellent stability and reproducibility, making them a valuable addition to SERS systems [10].

The search for a universal substrate for surface-enhanced Raman spectroscopy remains a challenge in the field of analytical chemistry [11-13]. The development of such a substrate proves to be a complicated endeavour, mainly due to the many SERS interactions between the analytes and the substrate surface. These interactions are highly dependent on factors such as the chemical composition, size, shape, and arrangement of the nanostructures of the substrate, making the development of a one-size-fits-all solution extremely difficult. The ultimate goal is to develop a simple and reproducible protocol that delivers highly efficient SERS substrates for a wide range of applications, simplifying the process and expanding the accessibility of this powerful analytical technique.

An important step in the production of nanostructures suitable for SERS applications is the process of forming silver nanoparticles on etched silicone surfaces. Ag NPs are formed on etched silicone surfaces by a combination of chemical and physical processes [14]. Etching creates a structured surface with an enlarged surface area that provides numerous nucleation sites for the deposition of silver ions. The reduction of the Ag ions to metallic silver nanoparticles is then initiated by a reducing agent, which is often introduced during the synthesis process. This reduction reaction is favoured by the high surface energy and reactivity of the etched silicone and leads to the formation of well-dispersed silver nanoparticles, which are used in various fields such as catalysis, electronics and biomedicine [15].

Melamine is a particularly interesting molecule as it has significant health and safety implications. It is a synthetic organic compound used in many industrial applications, including the manufacture of plastics, adhesives, and flame retardant materials [16]. It is best known for its involvement in several food safety incidents in which it was fraudulently added to dairy products to artificially increase protein content, resulting in significant health risks [17]. In its crystalline form, melamine is used in the manufacture of durable and heat-resistant tableware and kitchen utensils due to its exceptional heat and stain resistance. Consumption of or contact with melamine can have negative health effects [18]. It can form crystals or insoluble complexes in the urinary tract, especially when consumed with cyanuric acid or uric acid, which can lead to the formation of kidney stones and other kidney problems [19]. Chronic exposure to elevated levels of melamine can have long-term health consequences [20].

Recently, various sensors have been developed for the detection of melamine with low detection limits, including electrochemiluminescence sensors based on CNTs and CdSe@ZnSe, chemical sensors using ternary ZnO/CuO/Co_3O_4 nanoparticles and dimodal scattering spectral methods for rapid detection in dairy products [21-23]. In addition, SERS substrates made of sulphonated polystyrene microspheres coated with silver nanosheets have been developed to improve detection capability [24].

Nanoplastics (NPs), polymer particles with dimensions in the nanometre range, are widespread in the environment due to plastic pollution and material fragmentation [25-27]. They are now found in water, soil and the atmosphere, which is a cause for concern due to their potential for bioaccumulation [28-30]. While the methods for analysing microplastics are well established, the approaches for detecting nanoplastics are still incomplete. Raman microscopy and pyrolysis-gas chromatography–mass spectrometry have shown promise, as have new sensor technologies such as optical biosensors and SERS-based methods, which have demonstrated the ability to detect nanoplastics in various environmental samples [28, 31-33]. Despite these advances, a generally reliable method for the detection and quantification of nanoplastics has yet to be developed.

In this study, we investigate the deposition of silver and gold nanoparticles on silicon filters to develop a novel SERS substrate. The substrate was investigated with the standard probe molecule 4-mercaptobenzoic acid (4-MBA) as well as with melamine and various nanometre-sized polymers. The combination of the plasmonic properties of Ag and Au nanoparticles with the patterned surface features of Si filters creates a platform for the amplification of Raman signals from analytes of interest. This work addresses the growing need for adaptable and high performance SERS substrates that have potential applications in environmental monitoring, chemical sensing and biomedical diagnostics.

2. Materials and methods

2.1. Materials

Hydrofluoric acid (HF, 48%), melamine and 4-mercaptobensoic acid (4-MBA) were provided by Merck (USA) and silver nitrate and ethanol by Gram-mol (Croatia). Polystyrene spheres with diameters of 200, 350 and 1000 nm (all 2.5% (w/v) in water) were purchased from Polysciences, Inc (USA). PE microparticles with an average size of 65 nm were purchased from Lab261 (USA). The nanoplastic particles are dispersed in water, but before they were applied to the various substrates, they were further diluted with ultrapure water to obtain a known number of nanoparticles on the substrates. Macroporous silicon lift-off membranes (Si filters) with a pore diameter of 1 µm and a pore length of 200 µm were supplied by Smart Membranes (Germany). High purity water (18 MΩ cm^{-1}) was used for all experiments. All chemicals were of analytical purity.

2.2. Preparation of Ag coated Si filters

Silicon filters (10 × 10 mm) with pores of 1 µm diameter were washed with ethanol and immersed in a hydrofluoric acid : ethanol = 1 : 3 solution. After 60 seconds, the filters were thoroughly rinsed with ethanol and immersed in a 0.01 M $AgNO_3$ solution for a specified time (15 and 30 seconds, 1, 2, 3, 4, 15, 30 and 60 min). After immersion, the filters were rinsed with water and dried in air in the laminar flow.

2.3. Preparation of Au coated Ag-Si samples

The substrates were decorated by sputtering Au in the Polaron E5000 sputter coater under constant Ar flow. Based on previous measurements, the corresponding Au layer thicknesses were approximately 7 nm (3 min), 14 nm (6 min) and 21 nm (9 min).

2.4. Preparation of SERS samples

After deposition, the filters were carefully cut into squares of about 2 × 2 mm. Suitable concentrations of 4-MBA were obtained by dissolving in ethanol. Melamine was dissolved in water. The SERS substrates were soaked in a suitable 4-MBA solution for at least 10 minutes. The nanoplastic particles were diluted in ultrapure water. 2 µL of the solution of the nanoplastic particles to be analysed was dropped onto the surface of the substrate and the drop was allowed to dry. The samples were prepared in laminar flow and analysed under the microscope of the Raman spectrometer.

2.5. Micro Raman spectroscopy

A Renishaw InVia^{TM} Raman spectrometer (Renishaw Plc, Wotton-under-Edge, UK) with a 532, 633 and 785 nm laser was used for the measurements. At the start of each experiment the spectrometer was calibrated with an internal Si sample measured at 520 cm^{-1}. The Raman spectra were recorded at room temperature. The power of the laser was set as high as possible without burning the sample. The spectra were recorded with a 50× or 100× objective as a map on a selected area with a specific step size and recording time. For a 532 nm laser with a 50x objective, the size of the laser spot was ~0.87 µm (NA = 0.75) and for the 100x objective ~0.76 µm (NA = 0.85). The size of the laser spot for the 785 nm laser was 1.1 µm for a 100x objective with an NA of 0.85.

For all measurements on Ag-Au coated substrates a laser excitation of 785 nm was used, the objective was 100× and the exposure time was 1 s. At least six maps were created for each type of polymer and each particle size. Some measurements covered large areas, and in this case the step size was set to 2 microns to achieve a reasonable measurement duration. Therefore, the resolution was not the same for all maps.

Peaks caused by cosmic rays were removed from the data and baseline correction was performed. In all cases, the Raman spectra of at least three randomly selected sample areas were measured on a specific substrate. Using the "Intensity at point" or "Signal to baseline" option, a map was created in which the most intense signal is highlighted in white, while black represents areas without a corresponding Raman band signal.

3. Results

3.1. SERS substrates with Ag coated filters

Figure 1 shows SEM images of the synthesised samples. It can be seen that the longer the filter is immersed in the 0.01 M $AgNO_3$ solution, the greater the silver coverage of the silicon surface. After an immersion time of 15 seconds, only a few Ag particles have formed. However, the sample with an immersion time of 30 seconds shows significantly better coverage with silver particles, even if the coverage is not uniform. The sample that was immersed for 2 minutes shows that a layer of silver crystals has formed in the pores of the filter and the diameter of the pores has become smaller. In the sample that was immersed for 3 minutes, the silver clogged the pores of the filter even more. Interestingly, the sample that was immersed for 4 minutes behaved differently to the samples described so far. The pores are not

so closed, but a thin layer has formed that seems to completely cover the entrance of some pores. When the sample is immersed for 15 minutes, another layer of silver appears to form, gaining height and covering the bottom layer. For the sample immersed for 30 minutes, the pores are largely closed and silver crystals of different sizes and shapes have formed. Surprisingly, after 60 minutes of immersion, the Ag nanoparticles have formed a layer at the edge of the pores, but have also grown together in certain areas to form larger structures. It also appears that in some pores there are fragments or broken off parts of a certain layer.

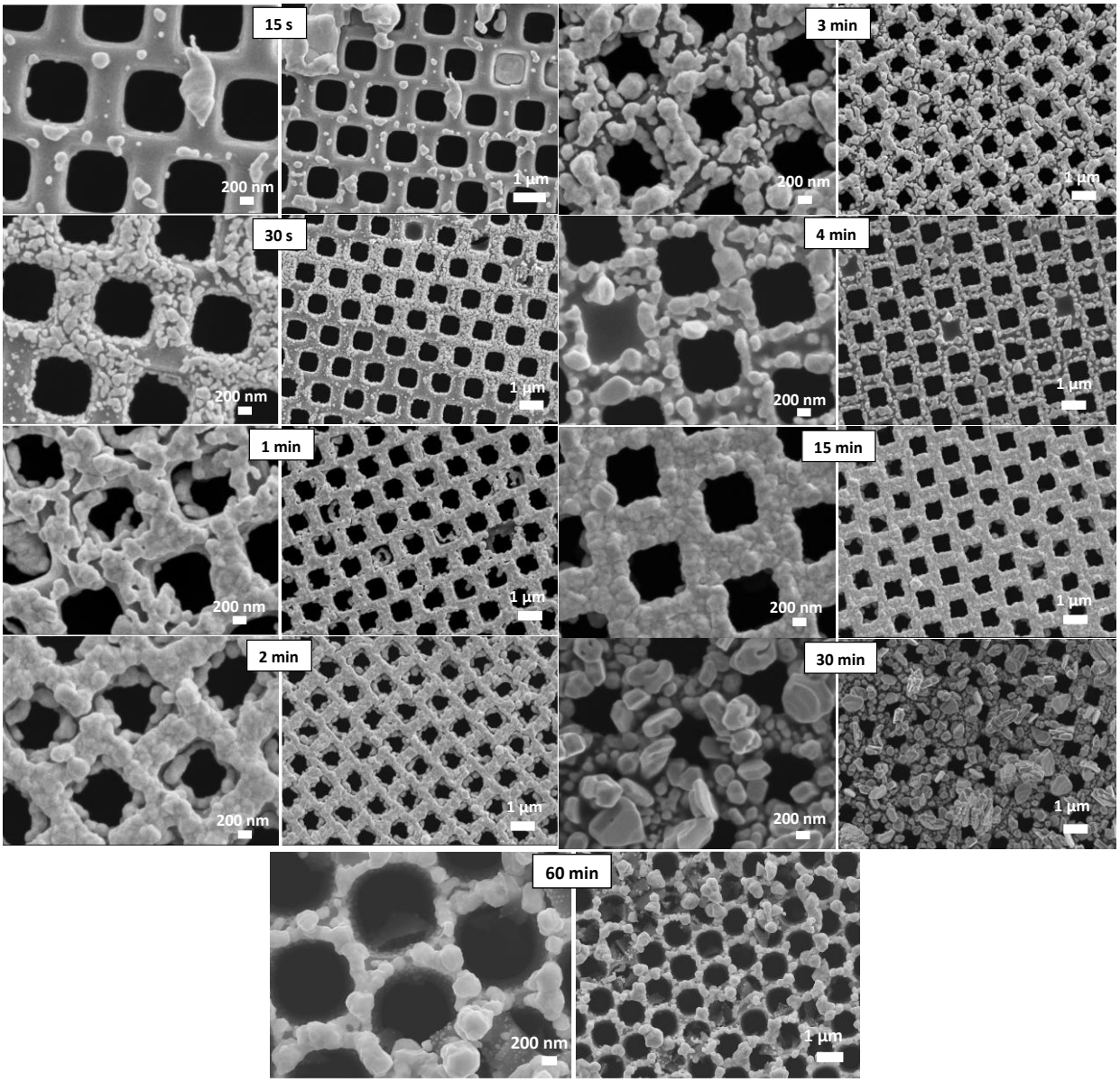

Figure 1. SEM images of synthesised Ag nanoparticles on the surface of Si filters after immersion in the $AgNO_3$ solution with different immersion times.

The substrates prepared in this way were tested for their SERS activity with 1 mM 4-mercaptobenzoic acid (4-MBA). Figure 2 shows the SERS spectra of 1 mM 4-MBA on Ag-coated Si filters prepared with different immersion times. The 4-MBA peak at 1585 cm^{-1} corresponds to fully symmetric C-C stretching, the peak at 1178 cm^{-1} to C-H deformation modes and the peak at 1078 cm^{-1} to in-plane ring breathing plus C-S stretching [34]. With increasing immersion time, the intensity of the Raman peaks also increases, which indicates a stronger amplification of the SERS signal with longer immersion. The most intense spectra were obtained at immersion times of 30 min and 60 min. The spectrum of the sample immersed for 1 min is slightly more intense and similar to the spectrum of the sample immersed for 15 min, but it is possible that this is due to the inhomogeneity of the sample itself.

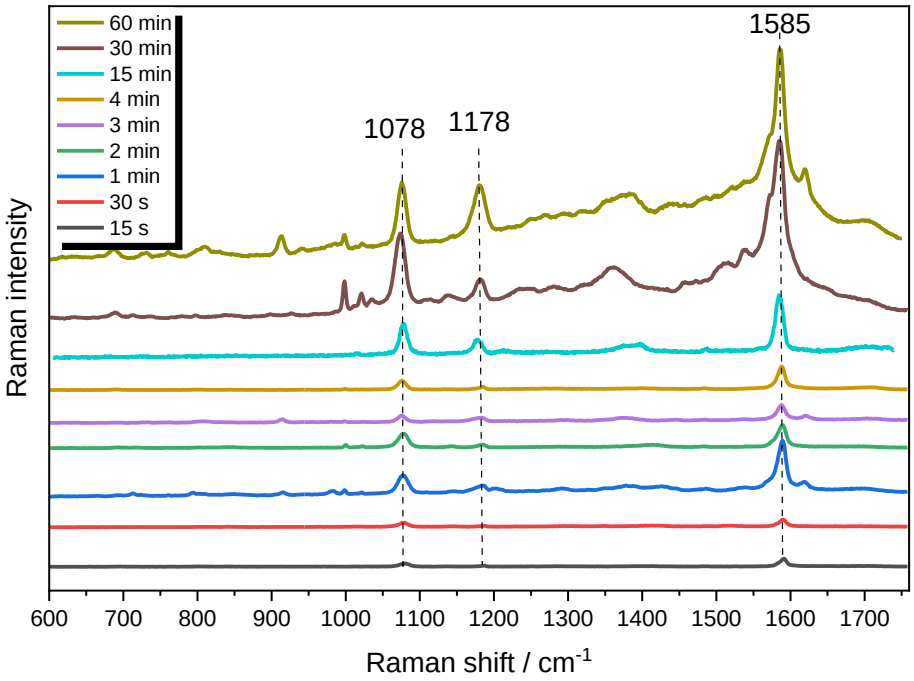

Figure 2. The SERS spectra of 1 mM 4-MBA on all prepared Ag-coated Si filters with different immersion times in 0.01 M $AgNO_3$ solution (15 and 30 s, 1, 2, 3, 4, 15, 30 and 60 min).

Figure 3 shows the SERS spectra of 4-MBA at different concentrations on Ag-coated Si filters prepared with different immersion times (4, 15, 30 and 60 min). The sample with an immersion time of 60 min shows the best detection performance, with clear spectral features even at low concentrations.

Thus, the best detection limit was achieved for the sample coated for 60 min and the 4-MBA spectrum at a concentration of 1 nM is clearly visible (Fig. 3d).

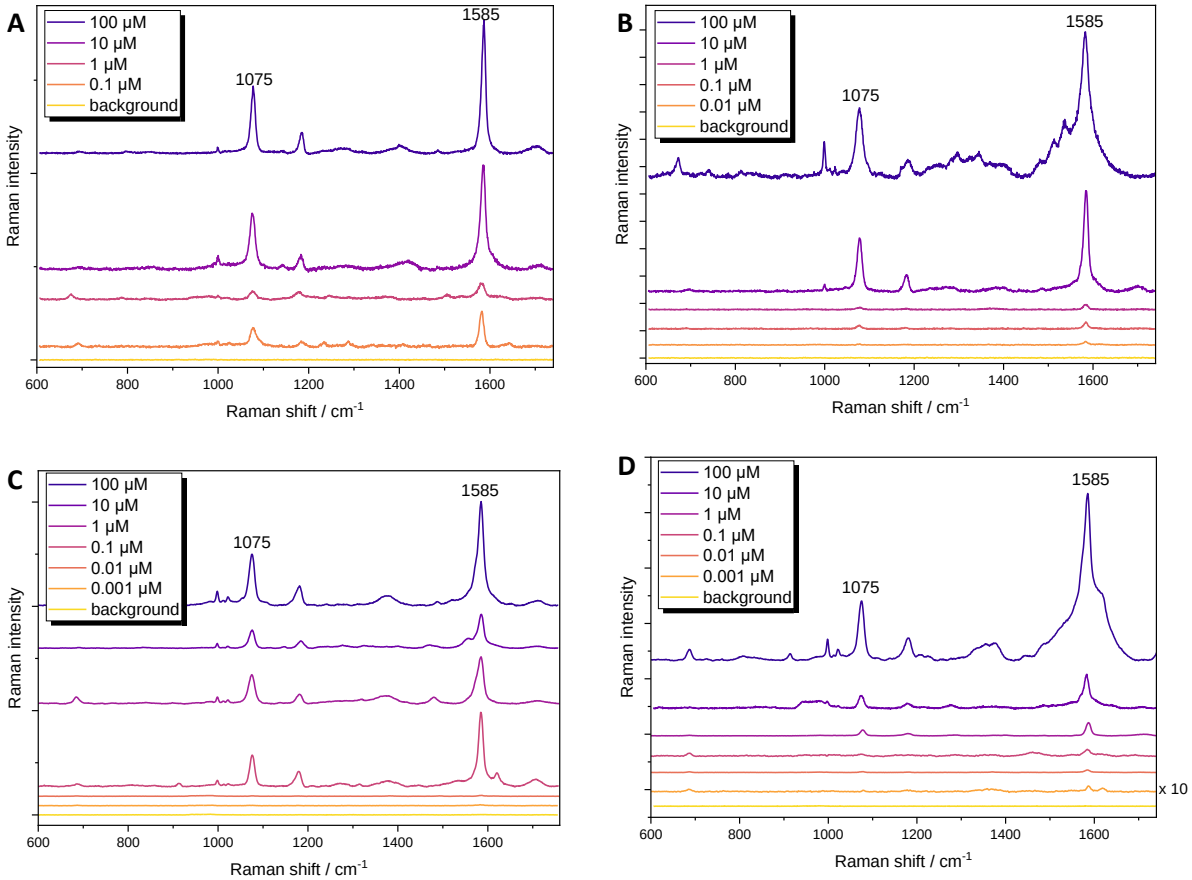

Figure 3. The SERS spectra of 4-MBA at different concentrations on Ag-coated Si filters with immersion times: a) 4, b) 15, c) 30 and d) 60 min.

The melamine analysis was carried out with the sample coated for 60 min and proved to be particularly suitable for the detection of 4-MBA. Figure 4 shows the Raman spectrum of the melamine powder, which exhibits intense bands at 676 and 984 cm^{-1} (breathing modes of the triazine ring) [35, 36]. The concentration of 0.01 M melamine on the Si substrate did not give a melamine spectrum, but only a silicon band at 520 cm^{-1}. A sample with 0.01 M melamine on a SERS substrate (Ag-immersion time 60 min) showed the melamine band at 684 (red shift by 8 wavenumbers) and 984 cm^{-1}, although the latter had a very low intensity. The wavenumber shift of the spectral bands in SERS is a characteristic feature due to the strong interaction between the substrate and the analyte [37]. The Raman shift of the 676 cm^{-1} band

is clear evidence of the adsorption of melamine on the Ag surface. It was also possible to detect a concentration of 1 mM melamine.

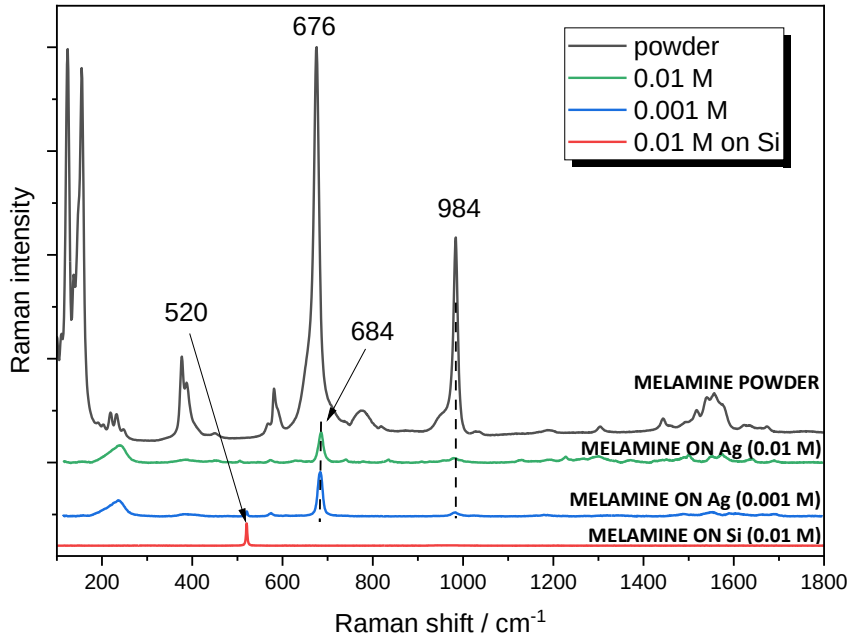

Figure 4. The Raman and SERS spectra of melamine. The SERS spectra were measured on Si-Ag coated 60 min.

3.2. SERS substrates with Au-Ag coated filters

Although silver has plasmonic properties that increase SERS sensitivity, it is very susceptible to oxidation, especially in an aqueous environment, which can affect its performance over time. Gold is known for its chemical stability and biocompatibility, which can improve the durability and functionality of the substrate. In addition, the combination of Ag and Au can lead to tunable surface plasmon resonance properties that enable more efficient and sensitive detection in SERS applications, especially in complex environments [38]. The SERS substrates obtained by gold sputtering for 3, 6 and 9 min are shown in Figure 5. Depending on the deposition time, different morphologies can be recognised. The size and distribution of the nanoparticles evolves with increasing deposition time, leading to conspicuous growth and aggregation patterns. At a deposition time of 6 min, a uniform distribution can be recognised, while larger clusters form with increasing exposure time. The weight percentage of gold in the samples produced was determined by EDX analysis (Table 1). It can be seen that the percentage of Au in the samples increases with increasing deposition time.

Table 1. The weight percentage of Au in the samples, determined by EDX.

min	Au	**average Au**
3 (spot 1)	37.43	38.40
3 (spot 2)	39.36	
6 (spot 1)	64.91	65.13
6 (spot 2)	65.35	
9 (spot 1)	72.48	72.99
9 (spot 2)	73.49	

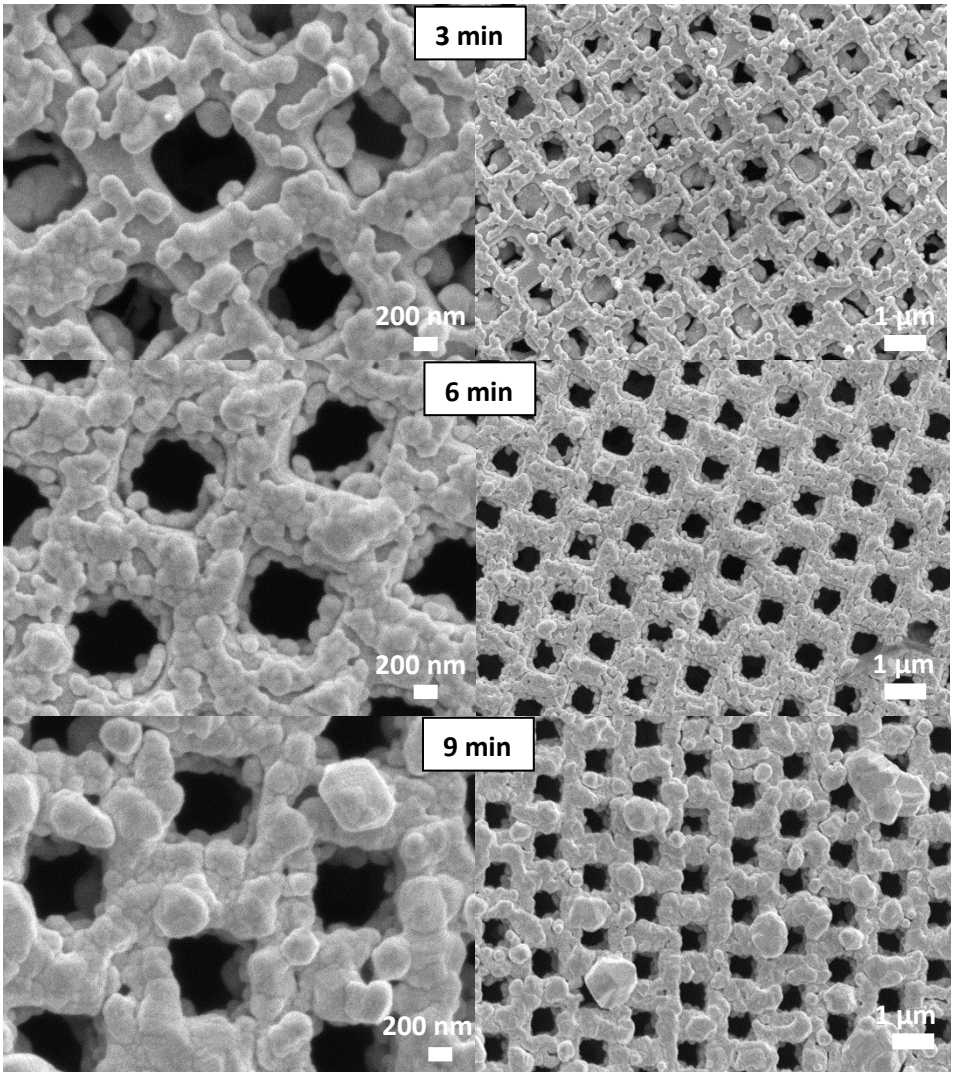

Figure 5. SEM images of Ag samples on the Si filters on which Au was deposited for 3, 6 and 9 minutes.

Figure 6a shows the SERS spectra of 1 mM 4-MBA on Au-Ag substrates with gold sputtering times of 3, 6 and 9 min. The peak positions are uniform (1077, 1182 and 1585 cm^{-1}), but the intensities of the peaks vary, showing the influence of the substrate morphology on the signal quality. In the concentration-

dependent spectra (Fig. 6b, c and d), we can see that the detection limits for the different substrates are also different. For all three samples, the most intense SERS bands were obtained at a concentration of 10 µM. While the band intensities for the samples with 3- and 9-minutes Au deposition times decrease sharply when the concentration is reduced tenfold, this is not the case for the sample with 6-minutes deposition time. For the substrate that was sputtered with Au for 6 min, the prominent peaks remain detectable down to the picomolar range (10^{-11} M).

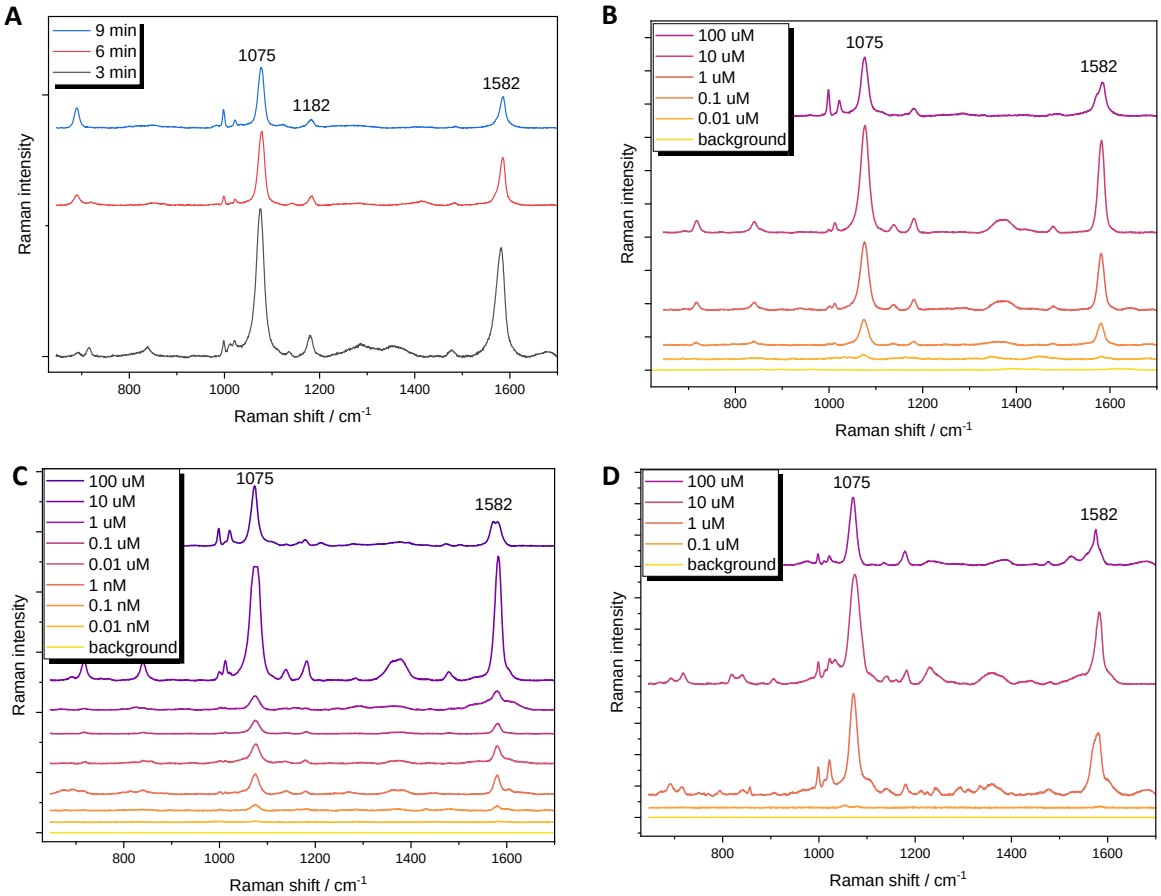

Figure 6. a) The SERS spectra of 1 mM 4-MBA on Au-Ag coated filters. 3, 6 and 9 min represent the three different evaporation times of the gold; 4-MBA at different concentrations on Au-Ag coated filters with deposition time: b) 3 min, c) 6 min and d) 9 min.

Figure 7 shows the SERS spectra for melamine obtained on substrates sputtered with gold for different periods of time. Fig. 7a shows the spectral response at a sputtering time of 3 min, while 7b shows the response at 6 min. The comparison shows how the deposition time influences the signal intensity and spectral quality. The detection limit for melamine is between 0.1 and 1 µM for the sample where Au was deposited for 6 min, while it is around 1 nM for the sample where Au was deposited for 3 min. The results

obtained are promising and comparable to those found in the literature [39, 40]. The main difference lies in the ease of preparation of our SERS substrate and the speed of analysis, which is a considerable advantage for practical applications.

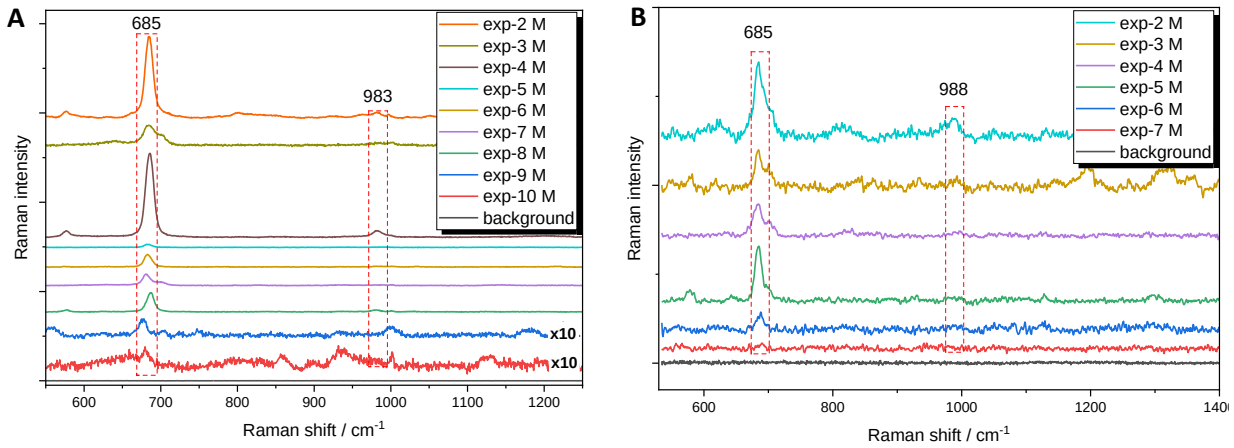

Figure 7. The SERS spectra of melamine measured on substrates sputtered with Au: a) 3 min and b) 6 min.

The difference in the optimal sputtering times for melamine and 4-MBA on SERS substrates is probably due to the different molecular interactions and resonance conditions on the substrate surface. For melamine, the 3-min Au sputtering sample yields a stronger SERS signal, suggesting that a thinner Au layer makes adsorption and the plasmonic field effect more effective for this particular molecule. In contrast, 6-min sputtering for 4-MBA likely provides a denser or continuous Au layer that better matches the molecular resonance conditions and results in better signal enhancement. This difference illustrates how the SERS response can be fine-tuned by tuning the sputtering duration to the specific analyte and its interaction with the plasmonic surface.

3.3. Micro-Raman analysis of nanoplastic particles on Au-Ag coated SERS substrates

Following the good results obtained in the analysis of melamine on SERS substrates, nanoplastic particles were also analysed. Analysing NPs using micro-Raman spectroscopy is a major challenge due to their small size and low scattering efficiency. The reduced Raman signal of NPs often leads to a poor signal-to-noise ratio, which limits the sensitivity of the technique. The fluorescence of polymer additives or degradation products can further obscure the Raman signals, making interpretation of the spectrum difficult. In addition, surface impurities or interactions with the environment can interfere with the

detection of characteristic molecular fingerprints. Finally, the small size makes the NP more susceptible to laser-induced degradation, which can compromise the integrity of the sample during analysis. It is obvious that polymer nanoparticles with smaller dimensions (e.g. 65 nm) can pass through the pores of our coated filters and therefore cannot be detected. However, the aim here was to attempt the detection of nanoplastics and thus set the direction for the further development of SERS substrates - namely to achieve a uniform surface with filled pores. However, if the goal is to filter liquid samples containing nanoplastics in order to subsequently detect them, this approach is a possible way to achieve this goal.

Several different polymers in commercially available sizes were selected for analysis: PS (1000, 350, 200 and 50 nm) and PE (65 nm). The samples were analysed by mapping the SERS substrate after applying a droplet containing the appropriate number of nanoplastic particles. A mapping review was then performed to determine if any of the spectra obtained matched the spectrum of the target polymer nanoparticles. All three gold substrates (3, 6 and 9 min) were tested and the results shown correspond to the best substrate for the respective polymer nanoparticles.

3.3.1. PS 1000, 350, 200 and 50 nm

Figure 8 shows the Raman mapping analysis performed to detect PS particles of different sizes (1000 nm, 350 nm, 200 nm and 50 nm) on the Au-Ag substrates. For the detection of polystyrene, the Raman peak at about 1002 cm^{-1} was used, which is due to the ring-breathing vibration [41]. For the 1000 nm PS particles (Fig. 8a), the Raman map shows distinct regions of high intensity, indicating the presence of PS. The 350 nm PS particles (Fig. 8b) show a similar mapping pattern, but with a slightly lower spatial resolution due to the smaller particle size and the larger mapping step size (1 µm). Nevertheless, the Raman spectrum still shows a clear signal at 1002 cm^{-1}. For the 200 nm PS particles (Fig. 8c), the mapping recognises smaller PS particles with a step size of 0.5 µm. The intensity map reflects the distribution of PS particles on the substrate, while the Raman spectrum retains the characteristic PS peaks, albeit with slightly lower intensity compared to larger particles. Finally, the 50 nm PS particles (Fig. 8d) show the sensitivity of the method for nanoscale particles. The higher laser power (5 %) and the higher accumulation (20) were necessary to improve the signal detection. The Raman map shows localised intensity hotspots indicating the presence of PS nanoparticles. The characteristic Raman peaks of PS are still observed, albeit with more noise, indicating the challenge of detecting such small particles with high precision. To evaluate the enhancement of the substrates, the 1000 nm PS spheres were analysed on pure Si filters without deposited Ag and Au. A Raman spectrum was obtained, but the intensity of the band at 1002 cm^{-1} is obscured by the silicon signal, making such measurements difficult (Fig. S1). A PS1000 signal

was also obtained on a sample on which Ag was deposited for 30 min, but the intensity of the band was weak (Fig. S2).

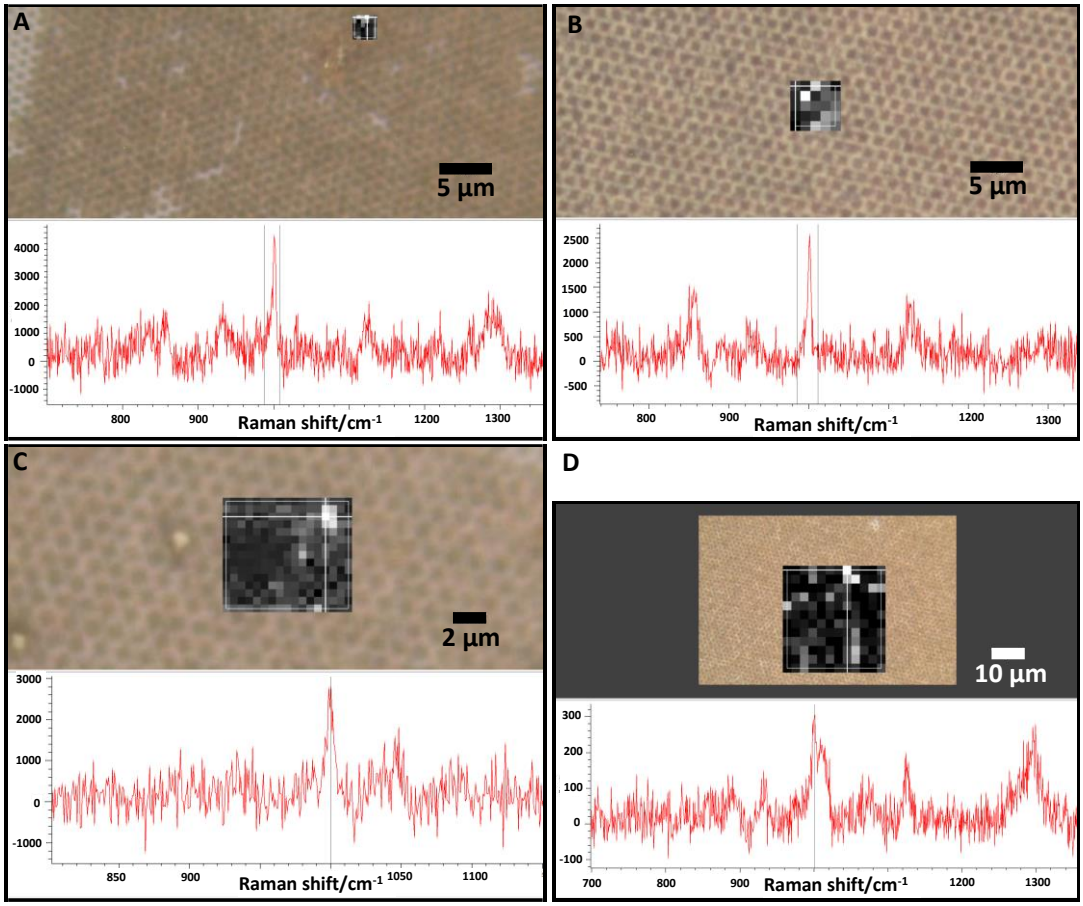

Figure 8. Mapping analysis of: a) PS 1000 nm (10 accumulations, laser power 1%, step 0.5, 6 min sample), b) PS 350 nm (10 accumulations, laser power 1%, step 1, 6 min sample), c) PS 200 nm (10 accumulations, laser power 1%, step 0.5, 6 min sample) and d) PS 50 nm (20 accumulations, laser power 5%, step 0.5, 9 min sample).

3.3.2. PE 65 nm

For polyethylene, the characteristic bands are 1462 cm^{-1} (CH_2 bending), 1439 cm^{-1} (CH_2 bending), 1294 cm^{-1} (CH_2 twisting), 1128 cm^{-1} (C–C stretching) and 1079 cm^{-1} (C–C stretching) [42]. Figure 9 shows the Raman mapping results of 65 nm PE nanospheres analysed on different SERS substrates. The grey-scale heat maps show variations in Raman signal intensity for the two bands at 1435 and 1460 cm^{-1}, with the lower panels showing representative spectra. Distinct peaks are observed around the characteristic Raman shifts of PE, revealing the molecular signature of the sample. Figure 10d shows the Raman spectrum of the PE standard and the spectra obtained by mapping on three different SERS substrates. The

characteristic bands of PE are labelled. A shift of four wavenumbers was observed for the bands at 1435 and 1458 cm^{-1}, which could be due to the broad nature of the bands or to variations in the local chemical environment and interactions with the substrate.

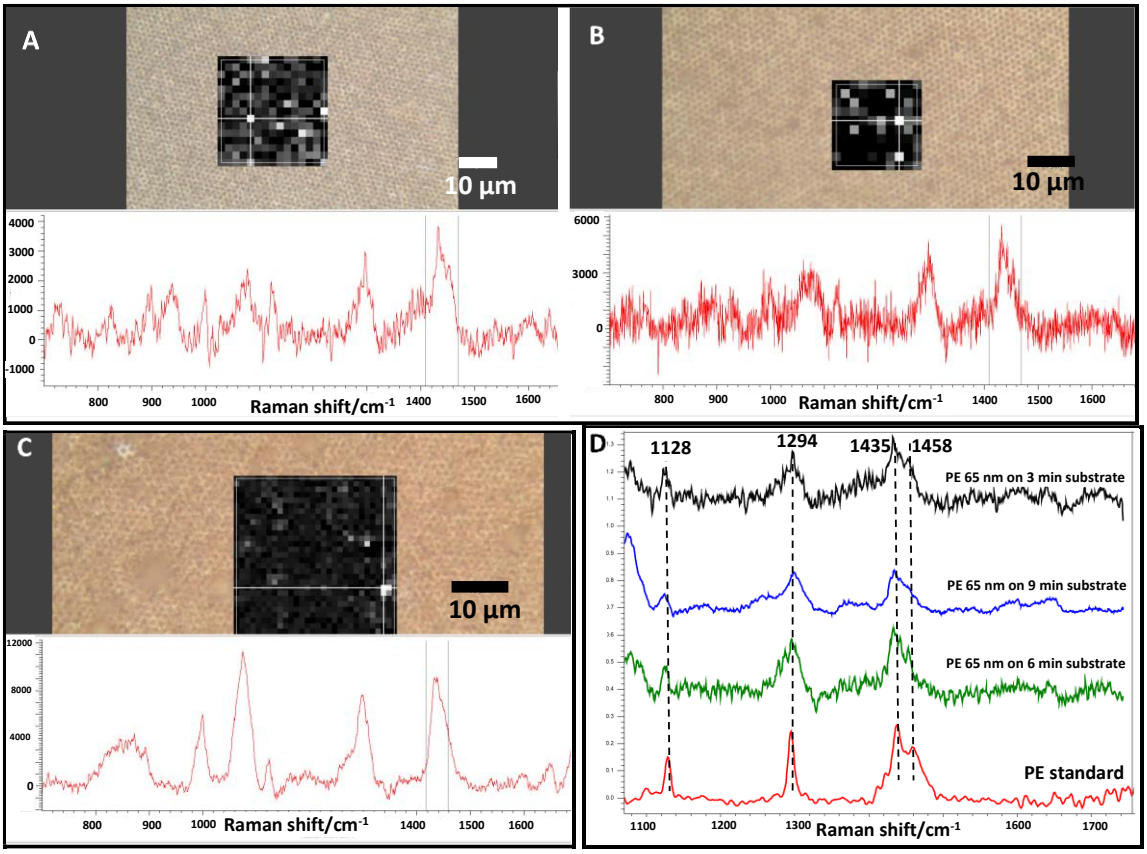

Figure 9. Mapping analysis: a) PE on Ag-Au 3 min sample (20 accumulations, laser power 5%, step 2), b) PE on Ag-Au 6 min sample (20 accumulations, laser power 5%, step 2) and c) PE on Ag-Au 9 min sample (20 accumulations, laser power 5%, step 1); d) PE spectra obtained on three different SERS substrates and spectrum of PE standard, with the characteristic polyethylene bands labelled.

We observed that shorter sputtering times (3 min) produced a stronger SERS signal for melamine, suggesting that a thinner gold layer enhances the plasmonic effects for this molecule. In contrast, a longer sputtering time (6 min) resulted in a continuous gold layer that was more effective for detecting molecules such as 4-MBA. These results are consistent with previous studies that emphasised the critical role of gold layer thickness in signal amplification [43, 44]. They show that SERS substrates can be tailored to optimise detection for specific analytes.

This study successfully demonstrates the detection of nanoplastics using SERS, overcoming the challenges posed by their small size and low scattering efficiency. Remarkably, we have achieved reliable

detection of nanoplastic particles as small as 50 nm. By adjusting the laser power and accumulation time, the signal quality was significantly improved, alleviating the inherent limitations of weak scattering on such small particles.

A major advantage of this approach is the simplicity and versatility of the SERS substrate fabrication process. Our method provides a cost-effective and efficient solution for the detection of nanoplastics and other contaminants that could have applications in various fields such as environmental monitoring, food safety and biomedical diagnostics. The ability to customise these substrates for specific detection requirements underlines their utility for rapid and reliable identification of small particles and paves the way for wider application in practise.

4. Conclusion

This study shows the successful synthesis and characterisation of Ag- and Au-Ag-coated silicon filter substrates for SERS applications. The immersion time of the Si filters in the $AgNO_3$ solution proved to be a critical factor influencing the morphology and distribution of the Ag nanoparticles as well as the resulting SERS activity. Short immersion times resulted in sparse Ag coverage, while longer immersion times led to uniform and dense nanoparticle layers that enhanced the SERS signal. The best SERS performance was achieved at an immersion time of 30–60 minutes, with the substrates showing high sensitivity for the detection of 4-MBA down to the nanomolar range.

The incorporation of gold by deposition further improved the performance of the SERS substrates. In particular, the Au-Ag substrates prepared with a 6-minute Au sputtering time showed optimal sensitivity and enabled the detection of 4-MBA at picomolar concentrations and melamine at micromolar concentrations. The results demonstrate the importance of matching Ag and Au deposition conditions to tailor the substrates for specific analytes and maximise detection performance.

The substrates were further tested for the detection of nanoplastic particles (PS and PE). This showed the potential for spatial mapping and molecular identification of nanoparticles down to 50 nm. Although the analysis of nanoplastics is challenging, the results underline the potential of optimised SERS substrates for the further development of nanoplastic detection, especially in environmental monitoring.

In summary, the developed Ag- and Au-Ag-coated SERS substrates exhibit excellent sensitivity, reproducibility and adaptability for various analytes, including small organic molecules and polymeric nanoparticles. Their simple manufacturing process combined with proven detection capabilities promises applications in chemical sensing, environmental analysis and beyond.

Acknowledgements

This work was financially supported by Croatian Government and the European Union through the European Regional Development Fund - the Competitiveness and Cohesion Operational Programme (KK.01.1.1.01.0001).

Literature

1. Han, X.X., R.S. Rodriguez, C.L. Haynes, Y. Ozaki and B. Zhao, Surface-enhanced Raman spectroscopy. *Nature Reviews Methods Primers*, **2022**. *1*(1): p. 87.
2. Sharma, B., R.R. Frontiera, A.-I. Henry, E. Ringe and R.P. Van Duyne, SERS: Materials, applications, and the future. *Mater. Today*, **2012**. *15*(1): p. 16-25.
3. Li, C., Y. Huang, X. Li, Y. Zhang, Q. Chen, Z. Ye, Z. Alqarni, S.E.J. Bell and Y. Xu, Towards practical and sustainable SERS: a review of recent developments in the construction of multifunctional enhancing substrates. *Journal of Materials Chemistry C*, **2021**. *9*(35): p. 11517-11552.
4. Chen, R. and L. Jensen, Interpreting the chemical mechanism in SERS using a Raman bond model. *The Journal of Chemical Physics*, **2020**. *152*(2).
5. Alonso-González, P., P. Albella, M. Schnell, J. Chen, F. Huth, A. García-Etxarri, F. Casanova, F. Golmar, L. Arzubiaga, L.E. Hueso, J. Aizpurua, and R. Hillenbrand, Resolving the electromagnetic mechanism of surface-enhanced light scattering at single hot spots. *Nature Communications*, **2012**. *3*(1): p. 684.
6. He, R.X., R. Liang, P. Peng and Y. Norman Zhou, Effect of the size of silver nanoparticles on SERS signal enhancement. *Journal of Nanoparticle Research*, **2017**. *19*(8): p. 267.
7. Pryshchepa, O., P. Pomastowski and B. Buszewski, Silver nanoparticles: Synthesis, investigation techniques, and properties. *Advances in Colloid and Interface Science*, **2020**. *284*.
8. Rycenga, M., P.H.C. Camargo, W. Li, C.H. Moran and Y. Xia, Understanding the SERS effects of single silver nanoparticles and their dimers, one at a time. *Journal of Physical Chemistry Letters*, **2010**. *1*(4): p. 696-703.
9. Ha, J.W., Strategies for sensitivity improvement of localized surface plasmon resonance sensors: experimental and mathematical approaches in plasmonic gold nanostructures. *Applied Spectroscopy Reviews*, **2023**. *58*(5): p. 346-365.
10. Yao, C., X. Zhang, C. Lu, Y. Liu, H. Li and C. Xie, High-performance SERS substrate based on gold nanoparticles-decorated micro/nano-hybrid hierarchical structure. *Materials Today Nano*, **2024**. *28*: p. 100525.
11. Gahlaut, S.K., A. Pathak and B.D. Gupta, Recent Advances in Silver Nanostructured Substrates for Plasmonic Sensors. *Biosensors*, **2022**. *12*(9).
12. Jebakumari, K.A.E., N.K. Murugasenapathi and T. Palanisamy, Engineered Two-Dimensional Nanostructures as SERS Substrates for Biomolecule Sensing: A Review. *Biosensors*, **2023**. *13*(1).
13. Lin, X.M., Y. Cui, Y.H. Xu, B. Ren and Z.Q. Tian, Surface-enhanced raman spectroscopy: Substrate-related issues. *Analytical and Bioanalytical Chemistry*, **2009**. *394*(7): p. 1729-1745.
14. Pinna, E., S. Le Gall, E. Torralba, G. Mula, C. Cachet-Vivier and S. Bastide, Mesopore Formation and Silicon Surface Nanostructuration by Metal-Assisted Chemical Etching With Silver Nanoparticles. *Frontiers in Chemistry*, **2020**. *8*.
15. Harraz, F.A., M. Faisal, A.E. Al-Salami, A.M. El-Toni, A.A. Almadiy, S.A. Al-Sayari and M.S. Al-Assiri, Silver nanoparticles decorated stain-etched mesoporous silicon for sensitive, selective detection of ascorbic acid. *Materials Letters*, **2019**. *234*: p. 96-100.

16. Emsley, A.M. and G.C. Stevens, *14 - The risks and benefits of flame retardants in consumer products*, in *Advances in Fire Retardant Materials*, A.R. Horrocks and D. Price, Editors. 2008, Woodhead Publishing. p. 363-397.
17. Tyan, Y.C., M.H. Yang, S.B. Jong, C.K. Wang and J. Shiea, Melamine contamination. *Analytical and Bioanalytical Chemistry*, **2009**. *395*(3): p. 729-735.
18. Mannoni, V., G. Padula, O. Panico, A. Maggio, C. Arena and M.R. Milana, Migration of formaldehyde and melamine from melaware and other amino resin tableware in real life service. *Food Additives and Contaminants - Part A Chemistry, Analysis, Control, Exposure and Risk Assessment*, **2017**. *34*(1): p. 113-125.
19. Hau, A.K.C., T.H. Kwan and P.K.T. Li, Melamine toxicity and the kidney. *Journal of the American Society of Nephrology*, **2009**. *20*(2): p. 245-250.
20. Lütjens, L.H., S. Pawlowski, M. Silvani, U. Blumenstein and I. Richter, Melamine in the environment: a critical review of available information. *Environmental Sciences Europe*, **2023**. *35*(1): p. 2.
21. Wu, Q., L. Tian, X. Shan, H. Li, S. Yang, C. Li and J. Lu, An electrochemiluminescence sensor based on the CNTs and CdSe@ZnSe for determination of melamine in milk samples. *Food Chemistry*, **2024**. *430*.
22. Alam, M.M., A.M. Asiri, M.T. Uddin, M.A. Islam, M.R. Awual and M.M. Rahman, One-step wet-chemical synthesis of ternary ZnO/CuO/Co3O4 nanoparticles for sensitive and selective melamine sensor development. *New Journal of Chemistry*, **2019**. *43*(12): p. 4849-4858.
23. Yi, C., A. Liang, G. Wen and Z. Jiang, A new difunctional liquid crystal nanosurface molecularly imprinted polyitaconic acid nanoprobe for SERS/RRS determination of ultratrace melamine. *Food Chemistry*, **2024**. *436*.
24. Chen, S., L. Chen, Y. Zhang, D. Xu, C. Hu, L. Zhang and J. Chen, Silver nanosheets self-assembled on polystyrene microspheres to form “hot spots” with different nanogap distances for high sensitive SERS detection. *Talanta*, **2024**. *268*.
25. Sangkham, S., O. Faikhaw, N. Munkong, P. Sakunkoo, C. Arunlertaree, M. Chavali, M. Mousazadeh and A. Tiwari, A review on microplastics and nanoplastics in the environment: Their occurrence, exposure routes, toxic studies, and potential effects on human health. *Marine Pollution Bulletin*, **2022**. *181*: p. 113832.
26. Pradel, A., C. Catrouillet and J. Gigault, The environmental fate of nanoplastics: What we know and what we need to know about aggregation. *NanoImpact*, **2023**. *29*: p. 100453.
27. Hale, R.C., M.E. Seeley, M.J. La Guardia, L. Mai and E.Y. Zeng, A Global Perspective on Microplastics. *J. Geophys. Res. Oceans*, **2020**. *125*(1): p. e2018JC014719.
28. Okoffo, E.D. and K.V. Thomas, Quantitative analysis of nanoplastics in environmental and potable waters by pyrolysis-gas chromatography–mass spectrometry. *Journal of Hazardous Materials*, **2024**. *464*.
29. Dube, E. and G.E. Okuthe, Plastics and Micro/Nano-Plastics (MNPs) in the Environment: Occurrence, Impact, and Toxicity. *Int J Environ Res Public Health*, **2023**. *20*(17).
30. O'Brien, S., C. Rauert, F. Ribeiro, E.D. Okoffo, S.D. Burrows, J.W. O'Brien, X. Wang, S.L. Wright and K.V. Thomas, There's something in the air: A review of sources, prevalence and behaviour of microplastics in the atmosphere. *Sci. Total Environ.*, **2023**. *874*: p. 162193.
31. Seggio, M., F. Arcadio, N. Cennamo, L. Zeni and A.M. Bossi, A plasmonic gold nano-surface functionalized with the estrogen receptor for fast and highly sensitive detection of nanoplastics. *Talanta*, **2024**. *267*.
32. Li, Z., K. Han, A. Zhang, T. Wang, Z. Yan, Z. Ding, Y. Shen, M. Zhang and W. Zhang, Honeycomb-like AgNPs@TiO2 array SERS sensor for the quantification of micro/nanoplastics in the environmental water samples. *Talanta*, **2024**. *266*.

33. Ruan, X., L. Xie, J. Liu, Q. Ge, Y. Liu, K. Li, W. You, T. Huang and L. Zhang, Rapid detection of nanoplastics down to 20 nm in water by surface-enhanced raman spectroscopy. *Journal of Hazardous Materials*, **2024**. *462*.
34. Pan, Y., W. Wang, S. Guo, S. Jin, E. Park, Y. Sun, L. Chen and Y.M. Jung *Charge Transfer on the Surface-Enhanced Raman Scattering of Ag/4-MBA/PEDOT:PSS System: Intermolecular Hydrogen Bonding*. Chemosensors, 2021. *9*, DOI: 10.3390/chemosensors9050111.
35. Yongliang, L., K. Chao, M.S. Kim, D. Tuschel, O. Olkhovyk and R.J. Priore, Potential of raman spectroscopy and imaging methods for rapid and routine screening of the presence of melamine in animal feed and foods. *Appl. Spectrosc.*, **2009**. *63*(4): p. 477-480.
36. Chen, X., Y. Hu, J. Gao, Y. Zhang and S. Li, Interaction of melamine molecules with silver nanoparticles explored by surface-enhanced Raman scattering and density functional theory calculations. *Appl Spectrosc*, **2013**. *67*(5): p. 491-7.
37. Yang, J.-L., Z.-W. Yang, Y.-J. Zhang, H. Ren, H. Zhang, Q.-C. Xu, R. Panneerselvam, K. Sivashanmugan, J.-F. Li and Z.-Q. Tian, Quantitative detection using two-dimension shell-isolated nanoparticle film. *Journal of Raman Spectroscopy*, **2017**. *48*(7): p. 919-924.
38. Wang, X., G. Ma, A. Li, J. Yu, Z. Yang, J. Lin, A. Li, X. Han and L. Guo, Composition-adjustable Ag-Au substitutional alloy microcages enabling tunable plasmon resonance for ultrasensitive SERS. *Chem Sci*, **2018**. *9*(16): p. 4009-4015.
39. Shameer, M., K. Vijai Anand, J. B.M Parambath, S. Columbus and H. Alawadhi, Direct detection of melamine in milk via surface-enhanced Raman scattering using gold-silver anisotropic nanostructures. *Spectrochimica Acta Part A: Molecular and Biomolecular Spectroscopy*, **2025**. *327*: p. 125412.
40. Kalambate, R.P., P.K. Kalambate and W. Laiwattanapaisal, Revolutionizing melamine detection: Cutting-edge advances from traditional analyses to state-of-the-art electrochemical sensors. *Next Materials*, **2024**. *3*: p. 100085.
41. Mikac, L., I. Rigó, L. Himics, A. Tolić, M. Ivanda and M. Veres, Surface-enhanced Raman spectroscopy for the detection of microplastics. *Appl. Surf. Sci.*, **2023**. *608*: p. 155239.
42. Furukawa, T., H. Sato, Y. Kita, K. Matsukawa, H. Yamaguchi, S. Ochiai, H.W. Siesler and Y. Ozaki, Molecular Structure, Crystallinity and Morphology of Polyethylene/Polypropylene Blends Studied by Raman Mapping, Scanning Electron Microscopy, Wide Angle X-Ray Diffraction, and Differential Scanning Calorimetry. *Polymer Journal*, **2006**. *38*(11): p. 1127-1136.
43. Magno, G., B. Belier and G. Barbillon, Gold thickness impact on the enhancement of SERS detection in low-cost Au/Si nanosensors. *Journal of Materials Science*, **2017**. *52*: p. 13650-13656.
44. Vilkevičius, K., I. Ignatjev, A. Selskis, G. Niaura and E. Stankevičius, Tuning SERS performance through the laser-induced morphology changes of gold nanostructures. *Applied Surface Science*, **2024**. *660*: p. 160003.